Serine 165 Phosphorylation of SHARPIN regulates the Activation of NF-κB

An Thys, Kilian Trillet, Sara Rosinska, Audrey Gayraud, Tiphaine Douanne, Yannic Danger, Clotilde Renaud, Luc Antigny, Régis Lavigne, Charles Pineau, et al.

▶ **To cite this version:**

An Thys, Kilian Trillet, Sara Rosinska, Audrey Gayraud, Tiphaine Douanne, et al.. Serine 165 Phosphorylation of SHARPIN regulates the Activation of NF-κB. 2020. hal-02991405

HAL Id: hal-02991405
https://hal.science/hal-02991405v1

Preprint submitted on 6 Nov 2020

HAL is a multi-disciplinary open access archive for the deposit and dissemination of scientific research documents, whether they are published or not. The documents may come from teaching and research institutions in France or abroad, or from public or private research centers.

L'archive ouverte pluridisciplinaire **HAL**, est destinée au dépôt et à la diffusion de documents scientifiques de niveau recherche, publiés ou non, émanant des établissements d'enseignement et de recherche français ou étrangers, des laboratoires publics ou privés.

bioRxiv preprint doi: https://doi.org/10.1101/2020.07.02.184085; this version posted July 3, 2020. The copyright holder for this preprint (which was not certified by peer review) is the author/funder. All rights reserved. No reuse allowed without permission.

Serine 165 Phosphorylation of SHARPIN regulates the Activation of NF-κB

An Thys[1], Kilian Trillet[1], Sara Rosinska[1], Audrey Gayraud[1], Tiphaine Douanne[1], Yannic Danger[2], Clotilde Renaud[1], Luc Antigny[1], Régis Lavigne[3,4], Charles Pineau[3,4], Emmanuelle Com[3,4], Franck Vérité[2], Julie Gavard[1,5], Nicolas Bidère[1,6]

[1] CRCINA, Inserm, CNRS, Université de Nantes, Université d'Angers, Nantes, France

[2] Etablissement Français du Sang (EFS), PFBI, Rennes

[3] Univ Rennes, Inserm, EHESP, Irset (Institut de recherche en santé, environnement et travail) - UMR_S 1085, Rennes, France

[4] Protim, Univ Rennes, Rennes, France

[5] Integrated Center for Oncology, ICO, St. Herblain, France

[6] Lead Contact

Running title:

SHARPIN phosphorylation regulates NF-κB

Keywords

LUBAC/NF-κB/phosphorylation/SHARPIN

Character count: 16,433

bioRxiv preprint doi: https://doi.org/10.1101/2020.07.02.184085; this version posted July 3, 2020. The copyright holder for this preprint (which was not certified by peer review) is the author/funder. All rights reserved. No reuse allowed without permission.

Abstract

The adaptor SHARPIN composes, together with the E3 ligases HOIP and HOIL1, the linear ubiquitin chain assembly complex. This enzymatic complex catalyzes and stamps atypical linear ubiquitin chains onto substrates to modify their fate, and has been linked to the regulation of the NF-κB pathway downstream most immunoreceptors, inflammation and cell death. However, how this signaling complex is regulated is not fully understood. Here, we report that a portion of SHARPIN is constitutively phosphorylated on the serine in position 165 in lymphoblastoid cells, and can be further induced following antigen receptor stimulation. Analysis of a phosphorylation-resistant mutant of SHARPIN revealed that this mark is dispensable for the generation of linear ubiquitin chains. However, phosphorylation allows the optimal activation of NF-κB in response to TNFα and T-cell receptor engagement. These results identify a new layer of regulation of the LUBAC, and unveil new strategies to modulate its action.

bioRxiv preprint doi: https://doi.org/10.1101/2020.07.02.184085; this version posted July 3, 2020. The copyright holder for this preprint (which was not certified by peer review) is the author/funder. All rights reserved. No reuse allowed without permission.

Introduction

The linear ubiquitin chain assembly complex (LUBAC) is an enzymatic triad of the adaptor SHARPIN (SHANK-associated RH domain-interacting protein) and the E3 ligases HOIP (HOIL-1 interacting protein, also known as RNF31) and HOIL-1 (RanBP-type and C3HC4-type zinc finger-containing protein 1, also called RBCK1, HOIL-1L) [1–3]. This unique complex catalyzes the formation and attachments of atypical linear ubiquitin chains on substrates, thereby modifying their fate. The LUBAC acts as a linchpin by transducing signals from most immunoreceptors to NF-κB, and therefore emerges as a key regulator of innate and adaptive immunity [1–13]. For instance, the binding of tumor necrosis factor α (TNFα) to its cognate receptor TNFR1 (TNF receptor 1) drives the recruitment of the LUBAC into the so-called complex I. By decorating the key protein kinase RIPK1 (receptor-interacting protein 1 kinase) with linear ubiquitin chains, the LUBAC stabilizes and favors downstream NF-κB signaling [1–3,7]. Mice deficient in SHARPIN, HOIP or HOIL-1 are hallmarked by an exacerbated TNFα induced cell death [1–3,14–16]. The loss of LUBAC components destabilizes this TNFR signaling complex I and induces the assembly of cytosolic complex II, causing cell death by apoptosis or necroptosis [1,14,15]. While, mice carrying a spontaneous SHARPIN-null mutation (*cpdm*) develop multi-organ inflammation and chronic proliferative dermatitis HOIP and HOIL-1 deficiency is embryonically lethal [1–3,14–16]. The LUBAC also functions downstream of antigen receptors to ensure the optimal activation of NF-κB, and this signaling pathway is pirated in the activated B cell like subtype of diffuse large B-cell lymphomas (ABC DLBCL) [17–20]. Accordingly, the targeting of the LUBAC was shown to be toxic in ABC DLBCL, unveiling a contribution of this complex to lymphomagenesis [19–22].

How the LUBAC is regulated continues to be elucidated. All members of the LUBAC have been reported to carry linear ubiquitin chains through auto-ubiquitination [23,24]. Recently, Iwai and colleagues demonstrated that HOIL-1 E3 ligase mono-ubiquitinates the LUBAC, which causes HOIP to preferentially decorate the LUBAC with linear ubiquitin chains rather

bioRxiv preprint doi: https://doi.org/10.1101/2020.07.02.184085; this version posted July 3, 2020. The copyright holder for this preprint (which was not certified by peer review) is the author/funder. All rights reserved. No reuse allowed without permission.

than other substrates [25]. Linear auto-ubiquitination of the LUBAC can be removed by the OTU deubiquitinase with linear linkage specificity (OTULIN) [23,24]. In addition, HOIP is processed upon TNFα- and TRAIL-induced apoptosis by caspases, with cleaved fragments displaying reduced NF-κB activation capabilities [26,27]. HOIP is also phosphorylated by mammalian ste20-like kinase 1 (MST1) in response to TNFα, and this modulates its E3 ligase activity, thereby attenuating NF-κB signaling [28]. Three independent groups, including ours, showed that HOIL-1 is cleaved by the paracaspase MALT1 upon antigen receptor engagement and constitutively in ABC DLBCL to allow optimal activation of NF-κB [29–31]. Lastly, SHARPIN is decorated with lysine (K) 63 ubiquitin chains in mice on K312. This ubiquitination was shown to be important for development of regulatory T cells [32]. However, what effect K63 ubiquitination of SHARPIN has on NF-κB signaling still remains an open question. Here, we demonstrate that a fraction of the LUBAC subunit SHARPIN is constitutively phosphorylated in lymphoblastoid cells, and this post-translational modification can be further induced upon antigen receptor engagement. We identify serine (S) 165 to be the primary phosphorylation site of SHARPIN, and provide evidence of its crucial role for the optimal activation of NF-κB response to both T-cell receptor engagement and TNFα stimulation.

Results and discussion

SHARPIN is a phosphoprotein

Western blotting analysis of SHARPIN, in human primary $CD4^+$ and $CD8^+$ cells, Jurkat cells and DLBCL cell lines, revealed that SHARPIN resolves as a doublet (Fig. 1A, EV1A). The treatment of cell lysates with lambda phosphatase, which removes phosphate groups from serine, threonine and tyrosine, effectively chased away the slow migration specie of SHARPIN, suggesting phosphorylation (Fig.1A, EV1A). Conversely, incubating cells with the phosphatase inhibitor Calyculin A resulted in an increase intensity of the slow migration

bioRxiv preprint doi: https://doi.org/10.1101/2020.07.02.184085; this version posted July 3, 2020. The copyright holder for this preprint (which was not certified by peer review) is the author/funder. All rights reserved. No reuse allowed without permission.

specie of SHARPIN, reinforcing the idea that SHARPIN is indeed phosphorylated (Fig. 1A). Quantification of constitutive SHARPIN phosphorylation in numerous cell lines, revealed that phospho-SHARPIN exists at various levels within different cell types, with lymphoid cells having a relatively high SHARPIN phosphorylation (Fig. 1B). Hence, a fraction of SHARPIN is constitutively phosphorylated.

Next, we determined whether stimuli, that employ SHARPIN, modify its phosphorylation. Mimicking antigen receptor engagement with phorbol 12-myristate 13-acetate (PMA) plus ionomycin increased the level of SHARPIN phosphorylation, which was efficiently removed by lambda phosphatase (Fig. 1C-D). This was however not the case for all activating stimuli. The change in SHARPIN phosphorylation was induced by PMA, but not ionomycin alone, cell stress inducer Anisomycin or TNFα stimulation (Fig. 1E, EV1B). SHARPIN phosphorylation is therefore specifically increased upon antigen receptor engagement. By comparing the signaling pathways ignited by these stimuli, we noticed that ERK activation was correlated with stimulation-mediated SHARPIN phosphorylation (Fig. 1E, EV1B). Incubating cells with the MEK1/2 inhibitor Trametinib prior to antigen receptor engagement, via PMA plus ionomycin or CD3 plus CD28 stimulation, brought SHARPIN phosphorylation back to basal levels, but did not prevent this constitutive mark (Fig. 1F, EV1C). By contrast, inhibition of the NF-κB pathway with the PKC inhibitor Bisindolylmaleimide VIII (BIMVIII) had no effect (Fig. 1F, EV1C). To gain molecular insights, HOIP, SHARPIN and ERK1-FLAG were overexpressed in HEKT293T cells. Co-immunoprecipitation of FLAG-tagged ERK1 showed an interaction between SHARPIN and ERK1, which was lost in the absence of HOIP (Fig. EV1D). Likewise, SHARPIN phosphorylation could be induced by recombinant ERK1 when the LUBAC is isolated through pulled down of the HOIL-1 subunit (Fig. EV1E). This indicates that SHARPIN requires the LUBAC complex in order to be phosphorylated by ERK1. However, while incubating cell lysates with lambda phosphatase entirely removed SHARPIN phosphorylation, ERK1/2 inhibition only brings SHARPIN phosphorylation back to control conditions (Fig. 1A, 1F). Hence, it seems that at least two kinases are involved in the

bioRxiv preprint doi: https://doi.org/10.1101/2020.07.02.184085; this version posted July 3, 2020. The copyright holder for this preprint (which was not certified by peer review) is the author/funder. All rights reserved. No reuse allowed without permission.

phosphorylation of SHARPIN, one, yet unidentified, that phosphorylates SHARPIN in resting conditions, and ERK1/2, which phosphorylates SHARPIN upon antigen receptor engagement.

Serine 165 is the major phospho-acceptor site within SHARPIN

Mass spectrometry of SHARPIN, purified by SHARPIN immunoprecipitation of untreated Jurkat cells, was conducted to identify putative phosphorylation sites. In total, 20 peptides were recognized as SHARPIN, covering 45.5% of the protein sequence (Fig. EV2A). Five phosphorylated peptides were identified, and five phosphorylation sites were detected on S129, S131, S146, S165 and S312, with a probability of 65.20%, 50%, 92,44%, 100% and 89.49%, respectively (Fig. 2A, EV2B). Out of the 5 serines identified, S165 and S312 were the most conserved ones across species (Fig. 2B). To explore the details of SHARPIN phosphorylation, we engineered a stable Jurkat cell line deficient in *Sharpin* using the CRISPR/Cas9 technology (Fig. EV2C-D). Jurkat *Sharpin* knockout cells were subsequently rescued with an empty vector (EV), wild type (WT) SHARPIN, or phospho-dead mutants of putative SHARPIN phosphorylation sites (S165A, S312A, S165A+S312A (2SA)). S165 SHARPIN and 2SA SHARPIN mutants, in both unstimulated and stimulated conditions, had a faster migration in SDS-PAGE of SHARPIN than the WT or S312A SHARPIN (Fig. 2C, EV2E). This implicates S165 to be the main phosphorylation site of SHARPIN. Western blotting analysis with a phospho-specific S165 (p-S165) SHARPIN antibody, after immunoprecipitation of SHARPIN, confirmed that SHARPIN is constitutively phosphorylated and that this phosphorylation can be further induced upon PMA plus ionomycin activation while it remains unaffected by TNFα stimulation (Fig. 2D).

As previously reported [1–3,14,33], the stability of LUBAC is compromised in SHARPIN deficient cells, which results in a diminished NF-κB activation as observed by NF-κB reporter luciferase assay (Fig. EV2D, EV2F). Rescuing Jurkat *Sharpin* knockout cells with WT, S165A

bioRxiv preprint doi: https://doi.org/10.1101/2020.07.02.184085; this version posted July 3, 2020. The copyright holder for this preprint (which was not certified by peer review) is the author/funder. All rights reserved. No reuse allowed without permission.

or phospho-mimetic S165D SHARPIN resulted in a replenishment of the LUBAC components HOIP and HOIL-1 (Fig. 2E), in a similar manner than the parental cells (Fig. EV2G). Hence, SHARPIN phosphorylation had seemingly no effect on the composition of the LUBAC (Fig. 2F).

SHARPIN phosphorylation contributes to the optimal activation of NF-κB

The LUBAC is recruited to the TNFR1 complex I upon TNFα stimulation, where it is crucial for stabilizing the complex and subsequent NF-κB activation. It does so by modifying components of the TNFR1 complex I, including RIPK1, with linear ubiquitin (Methionine-1, M1) chains. This allows for a more efficient recruitment and retention of the IκB kinase (IKK) complex, consisting of IKKα, IKKβ and NEMO, with NEMO itself being modified with M1-chains. When activated, the IKK complex phosphorylates NF-κB inhibitors IκBs leading to their degradation. This liberates NF-κB to translocate into the nucleus where it can fulfill its transcription factor function [1–3,7,34]. Loss of LUBAC components leads to a switch from complex I to complex II, thereby inducing cell death by apoptosis or necroptosis [1,14,15]. We therefore studied the effect of SHARPIN phosphorylation on cell viability following TNFα stimulation. As previously shown [1–3], TNFα stimulation of *Sharpin* knockout cells reconstituted with an empty vector effectively reduced cell viability, while reconstitution with WT-, S165A-, or S165D-SHARPIN resulted in a similar protective effect against TNFα (Fig.3A). Even though phosphorylated SHARPIN is detected at the TNFR1, upon TNFα-FLAG stimulation (Fig. EV3A), recruitment of the phospho-dead SHARPIN to the TNFR1 complex I was normal, as was M1 ubiquitination at the TNFR1 receptor (Fig. EV3B). Likewise, TNFα stimulation did not drive any significant changes in total M1 ubiquitination or linear ubiquitination of the known substrate RIPK1 (Fig. 3B). Activation of immune cells by antigen receptor engagement leads to the assembly of a signaling complex of CARMA1, BCL10 and MALT1 (coined CBM complex). This complex serves as docking site for the LUBAC, which authorizes the recruitment and activation of IKK [17–19,33,35]. Within this

bioRxiv preprint doi: https://doi.org/10.1101/2020.07.02.184085; this version posted July 3, 2020. The copyright holder for this preprint (which was not certified by peer review) is the author/funder. All rights reserved. No reuse allowed without permission.

signaling platform, the paracaspase MALT1 cleaves HOIL-1 [29–31]. We found that the phosphorylation status of SHARPIN did not influence the capability of MALT1 to cleave HOIL-1 upon antigen receptor engagement (Fig. 3C), implicating a normal assembly of the CBM complex. Furthermore, IκBα phosphorylation was unchanged in cells stimulated with TNFα or with PMA plus ionomycin (Fig. EV3C-D). Altogether; these results suggest that SHARPIN does not affect the recruitment of the LUBAC to the TNFR1 or CBM complexes, nor its ability to catalyze M1 chains and promote IKK activation.

Nonetheless, SHARPIN phosphorylation emerged as a key player in the optimal activation of NF-κB (Fig. 3D-G). NF-κB family members control the transcription of cytokines, and regulate cellular differentiation, survival and proliferation [36]. The NF-κB family is composed of five related transcription factors in mammals: p50, p52, p65 (also called RelA), c-Rel and RelB [37]. As expected, the transcription activity of NF-κB, as measured by a NF-κB reporter luciferase assay, was reduced in *Sharpin* knockout cells, reconstituted with an empty vector, stimulated through antigen receptor engagement or TNFα, when compared to cells expressing WT-SHARPIN (Fig. 3D). Interestingly, NF-κB activity was restored in cells expressing S165D-SHARPIN, but not S165A-SHARPIN (Fig. 3D), unveiling a key role for S165 phosphorylation. Likewise, cells expressing S165A-SHARPIN displayed a reduced DNA binding of the NF-κB subunits p65 and p50 upon antigen receptor engagement or TNFα stimulation (Fig. 3E). Of note, the binding of c-Rel was unchanged (Fig. EV3E), whereas p52 and RelB signals did not reach the threshold limits (data not shown). In keeping with these results, PCR array of human NF-κB signaling targets showed a significant diminished expression of numerous cytokines (CSF3, IL12B, IFNBA, IL6, CXCL9, CCL22, IL2 and IL4) and chemokines (CXLCL1, CXCL2, CXCL8, CCL11) in S165A-SHARPIN expressing cells treated with PMA and ionomycin (Fig. 3F, Fig. EV3F). Similar results were found when cells were stimulated with TNFα, albeit only the chemokine receptor CXCR2 reached statistical significance there is a trend towards reduced expression of other NF-κB signaling targets

bioRxiv preprint doi: https://doi.org/10.1101/2020.07.02.184085; this version posted July 3, 2020. The copyright holder for this preprint (which was not certified by peer review) is the author/funder. All rights reserved. No reuse allowed without permission.

(Fig. 3G, EV3G). It should be mentioned that compared to PMA plus ionomycin stimulation, induction of NF-κB target genes by TNFα was weaker, which may also explain why differences upon TNFα stimulation are less striking. Nevertheless, we established that the phosphorylation of SHARPIN on S165 is participates in NF-κB upon antigen receptor engagement and TNFα stimulation.

In summary, we have discovered that a part of SHARPIN is constitutively phosphorylated in lymphoblastoid cells and identified S165 as the main phospho-acceptor residue. We also provide evidence that SHARPIN is further phosphorylated on the Serine 165 by ERK upon antigen receptor engagement, but not in response to TNFα (Fig. 1C). Yet, the constitutive phosphorylation of SHARPIN is pivotal for the optimal activation of NF-κB in response to antigen receptor engagement and TNFR ligation. This apparent dichotomy militates against a role for the inducible phosphorylation in NF-κB activation. It is therefore tempting to speculate that ERK-mediated phosphorylation of SHARPIN plays an independent function. Beside its crucial role in NF-κB signaling, a growing body of literature suggests that SHARPIN also acts as an inhibitor of the integrin adhesion receptors [38–40]. Pouwels *et al.* demonstrated that SHARPIN locates at and controls the detachment of cellular protrusions called uropods in lymphocytes, and that this is essential for lymphocyte movement [39]. As antigen receptor engagement delivers a stop signal to migrating T lymphocytes [41–43], ERK-dependent SHARPIN phosphorylation may have an impact on cell adhesion and migration. This description of at least two kinases targeting the same site, with different outcomes is reminiscent of what has been shown for MLKL (mixed lineage kinase domain-like pseudokinase). MLKL acute phosphorylation by RIPK3 at T357 and S358 triggers necrotic cell death [44], while basal phosphorylation on the same sites by a yet-to-be-defined kinase promotes the generation of small extracellular vesicles [45]. Lastly, the LUBAC may exist in different complexes, with different binding partners [46,47]. One could therefore

bioRxiv preprint doi: https://doi.org/10.1101/2020.07.02.184085; this version posted July 3, 2020. The copyright holder for this preprint (which was not certified by peer review) is the author/funder. All rights reserved. No reuse allowed without permission.

speculate that different kinases could target different LUBAC complexes, and consequently exert selective functions.

Although necessary for complete NF-κB activity upon antigen receptor engagement and TNFα stimulation, how SHARPIN phosphorylation regulates the LUBAC functions and NF-κB signaling is unclear. The basal S165 SHARPIN phosphorylation appeared dispensable for TNFα-induced cell death, linear ubiquitination, assembly of CBM or TNFR1 complexes, and IKK activation. Additional work is therefore required to better understand this new layer of complexity in the regulation of NF-κB transcription activity. Nevertheless, this may also open up new avenues for therapeutic prospects of aggressive lymphoma, such as ABC DLBCL, for which the LUBAC and NF-κB activation is pivotal for survival [19,33]. *Hoip* and *Sharpin* deficiency in mice results in embryonic lethality or multiorgan inflammation, respectively, which is driven by aberrant TNFα-induced cell death [14,15,48–50]. Directly targeting SHARPIN phosphorylation for treatment may therefore circumvent the pitfall of inducing autoinflammatory diseases while targeting the NF-κB pathway specifically. The identification of the kinase responsible for constitutive SHARPIN phosphorylation will therefore be paramount to our future research.

Material and Methods

Cell culture

Jurkat E6.1 T lymphocytes, Hela, HEK293T and MCF7 cells were purchased from American Type Culture Collection (ATCC). U2932, SUDHL4, BJAB, RIVA, OCI-LY3, and OCI-LY19 cells were acquired from DSMZ. HBL1, HLY1 and TMD8 cells were kindly provided by Martin Dyer, Pierre Brousset, and Daniel Krappmann, respectively. Blood was obtained from healthy donors (Etablissement Français du Sang). Peripheral blood mononuclear cells (PBMC) were acquired by Ficoll density gradient. Primary $CD4^+$ and $CD8^+$ T cells were

bioRxiv preprint doi: https://doi.org/10.1101/2020.07.02.184085; this version posted July 3, 2020. The copyright holder for this preprint (which was not certified by peer review) is the author/funder. All rights reserved. No reuse allowed without permission.

subsequentially isolated from PBMC using REAlease CD4 and CD8 microbeads kits, from Miltenyi as manufacturer's instructions. Cell viability was assessed using CellTiter-Glo following manufacturer's instructions (Promega) following stimulation with 10 ng/mL TNFα (R&D systems) for 24h.

Immunoblotting

Jurkat E6.1, PBMC or primary T cells were stimulated with 20 ng/mL Phorbol 12-Myristate 13 Acetate (PMA, Merck), 300 ng/mL ionomycin (Merck), PMA plus ionomycin, 1 μg/mL CD3 plus 1 μg/mL CD28 (Becton Dickinson Biosciences), 12.5 mg/mL anisomycin (Merck), 10 ng/mL TNFα (R&D systems) or TNFα-Flag (Enzo Life Sciences). To ensure inhibition of certain signaling pathways Jurkat E6.1, PBMC or primary T cells were pre-treated during 1h with 1 μM Trametinib (Selleckchem), 500 nM Bisindolylmaleimide VIII (BIMVIII, Enzo), 50 μM SP6000125 (Cell Signaling), or 5 μM SB203580 (Selleckchem). Cells were washed with ice-cold PBS and subsequently lysed using two possible lysis buffers, as indicated throughout the manuscript. (1) Cells pellets were incubated with 188 μl of Buffer A (10 mM HEPES pH7.9, 10 mM KCL, 0.1 mM EDTA, 0.1 mM EGTA, 1mM DTT and 1 mM Na_3VO_4) for 5 min on ice. 12 μl of Buffer A containing 10% Igepal was added for another 5 min on ice and samples were subsequently centrifuged at 1,000 g for 3 min. Supernatant was collected. (2) Cell pellets were lysed with TNT buffer (50 mM Tris-HCl (pH 7.4), 150 mM NaCl, 1% Triton X-100, 1% Igepal, 2 mM EDTA), and incubated for 30 min on ice. Extracts were cleared by centrifugation at >10 000 x g. Lysis buffers were supplemented with 1x Halt Protease Inhibitor cocktail (ThermoFisher Scientific). Protein concentration was determined using the Micro BCA Protein Assay kit (ThermoFisher scientific), for both lysis buffers. Lambda phosphatase experiments used either Buffer A or TNT lysis without EDTA or EGTA for cell lysis. 10 μg of protein was incubated with 600 Units of lambda phosphatase, 1x NEB buffer for Protein Metallophosphatase and 1mM $MnCl_2$ (New England Biolabs) for 30 min at 30°C.

bioRxiv preprint doi: https://doi.org/10.1101/2020.07.02.184085; this version posted July 3, 2020. The copyright holder for this preprint (which was not certified by peer review) is the author/funder. All rights reserved. No reuse allowed without permission.

10 µg of proteins was incubated with 2X Laemmli buffer (Life Technologies) at 95°C for 3 min, separated by SDS-PAGE using a 3-15% Tris-Acetate gel and transferred to nitrocellulose membranes (GE Healthcare). Densitometry analysis was performed by the Image J software (National Institutes of Health).

The following antibodies were used for analysis by immunoblot: SHARPIN (A303-559A), HOIP (A303-560A), and IκBβ (A301-828A) antibodies were purchased from Bethyl. HOIL-1 (sc-393754), αTubulin (sc-8035), CYLD (sc-137139) and GAPDH (sc-32233) antibodies were obtained from Santa Cruz Biotechnology. Phospho-ERK (#9106), IκBα (#9242), phospho-IκBα (#9246), phospho-p38 (#9215), phospho-JNK (#9255) and RIP1 (#3493) were acquired from Cell Signaling Technologies. Anti-linear Ubiquitin (MABS199) was procured from Millipore. For detection of the phospho-S165 from of human SHARPIN, five Balb/C mice were primed via intraperitoneal injection with complete Freund adjuvant and boosted two times at two-week intervals with incomplete Freund adjuvant with a synthetic phosphorylated peptide (DLPR(Sp)PGNLTERC) conjugated to KLH. Mouse blood was collected from the submandibular vein and serum reactivity was confirmed by ELISA with phosphorylated and non-phosphorylated biotinylated peptide. Mouse serum was used to reveal phospho-S165 SHARPIN.

Immunoprecipitation (IP) and ERK recombinant kinase assay

Cells were washed with ice-cold PBS, lysed with TNT buffer and incubated for 30 min on ice. Extracts were cleared by centrifugation at >10,000 g. Protein concentration was determined using the Micro BCA protein kit. Samples were precleared with Protein G Sepharose (Merck) for 30 min, and subsequently incubated with 1 µg of antibody and protein G Sepharose for a duration of 2h. Flag pull down was performed incubating cleared cell lysates with Anti-flag M2 affinity gel (Merck) during 2h. SHARPIN (A303-559A, Bethyl), HOIL-1 ((sc-393754, Santa Cruz Biotechnology) and linear ubiquitin, kindly provided by VM Dixit (Genentech), antibodies were used for IP. ERK1/2 kinase assay was performed from beads immunoprecipitated for

bioRxiv preprint doi: https://doi.org/10.1101/2020.07.02.184085; this version posted July 3, 2020. The copyright holder for this preprint (which was not certified by peer review) is the author/funder. All rights reserved. No reuse allowed without permission.

306 HOIL-1. Beads were washed in kinase buffer (5 mM MOPS pH 7.2, 5 mM $MgCl_2$, 1 mM
307 EGTA, 0.4 mM EDTA, 0.05 mM DTT). Beads were subsequently incubated with kinase
308 buffer, 2mM ATP, 350 ng/mL active untagged ERK1 (Merck), 350 ng/mL active ERK2-GST
309 tagged (Merck) or 175 ng/mL ERK1 plus 175 ng/mL ERK2-GST for 30 min at 30°C.
310

311 ***Mass Spectrometry***

312 Jurkat E6.1 cells were lysed in TNT lysis buffer supplemented with 1x Halt protease inhibitor
313 cocktail. Immunoprecipitation of SHARPIN was performed as described above. Proteins
314 were separated by SDS-PAGE. The Colloidal Blue Staining kit (LC6025, Invitrogen) was
315 used to stain protein as per manufacturer's instructions. Gel was excised between 37 and 50
316 kDa, to ensure the presence of SHARPIN, and subsequently cut into smaller fragments.
317 Fragments were washed alternating between 100 mM Ammonium Bicarbonate and
318 Acetonitrile. Disulfide bonds of proteins were reduced, with using 65 mM DTT for 15 min at
319 37°C, and subsequently alkylated by 135 mM Iodoacetamide for 15 min at room
320 temperature. Enzymatic digestion of proteins was performed at 37°C overnight by incubating
321 the gel pieces in 25 ng/mL pH 8.5 trypsin solution (Sequenced Grade Modified Trypsin, ref
322 V511A, Porcine, Promega). Digested peptides were extracted by incubation in 70% and
323 100% acetonitrile for 20 min each. Peptide extracts were evaporated and afterward
324 reconstituted in 0.1% formic acid. Peptide extracts were analyzed by liquid nano-
325 chromatography (nanoLC) nanoElute coupled with a TimsTOF Pro mass spectrometer
326 (Bruker), as previous described by [51]. Generated peaks were analyzed with the Mascot
327 database search engine (MatrixScience version 2.5.01) for peptide and protein identification.
328 The peaks were queried simultaneously in the: UniprotKB Human (release 20191016, 20656
329 sequences) database and a decoy database that was interrogated in parallel to estimate the
330 number of false identifications and to calculate the threshold at which the scores of the
331 identified peptides are valid. Mass tolerance for MS and MS/MS was set at 15 ppm and 0.05
332 Da, respectively. The enzyme selectivity was set to full trypsin with one miscleavage allowed.

bioRxiv preprint doi: https://doi.org/10.1101/2020.07.02.184085; this version posted July 3, 2020. The copyright holder for this preprint (which was not certified by peer review) is the author/funder. All rights reserved. No reuse allowed without permission.

Protein modifications were fixed carbamidomethylation of cysteines, variable oxidation of methionine, variable phosphorylation of serine, threonine or tyrosine. Identified proteins are validated with an FDR < 1% at PSM level and a peptide minimum score of 30, using Proline v2.0 software [52]. Proteins identified with the same set of peptides are automatically grouped together. Analysis of post-translational modifications was also executed using Proline v2.0 Software. Localization confidence values for peptide ions were exported from Mascot [53] and a site probability is calculated for a particular modification according to the number of peptides confidently detected with this site modification.

CRISPR/Cas9 knock out and SHARPIN reconstituted cell lines

LentiGuide and LentiCRISPRv2 vectors (GeCKO, ZhangLab), were cloned to contain SHARPIN guide RNA (5‘ CACCGTGGCTGTGCACGCCGCGGTG 3’), as described before (Sanjana et al., 2014; Shalem et al., 2014). LentiCRISPRv2, together with the packaging vectors PAX2 and VSV-G, were transfected in HEK293T cells using a standard calcium phosphate protocol, as previously published [54]. Supernatant, containing the lentiviral particles, was collected after 48 h, and used to infect 10^6 Jurkat cells in presence of 8 μg/mL Polybrene (Santa Cruz Biotechnology). Jurkat cells expressing the LentiCRISPRv2 vector were selected by adding 1μg/mL Puromycin to their media, and subsequently dilution cloned. Single-cell clones were then picked and tested for functional Cas9 cutting of SHARPIN (Fig.EV2C). SHARPIN was cloned from a pCMV3flag9SHARPIN vector (Addgene), into a pCMH-MSCV-EF1a-puroCopGFP vector (SBI). Site directed mutagenesis was performed using the pCMH-MSCV-EF1a-puroCopGFP vector containing wild type (WT) SHARPIN, to substitute the serine (S) residues on 165 or/and 312 to an alanine (A) or an aspartic acid (D). CRISPR/Cas9 resistance was achieved by site directed mutagenesis of the PAM sequence on site 29, substituting an Arginine (AGG) to an Arginine (AGA).

bioRxiv preprint doi: https://doi.org/10.1101/2020.07.02.184085; this version posted July 3, 2020. The copyright holder for this preprint (which was not certified by peer review) is the author/funder. All rights reserved. No reuse allowed without permission.

NF-κB assays

NF-κB luciferase assay was performed as previously described [20,29]. DNA binding of the NF-κB subunits was measured using TransAM NF-κB activation assay (Actif Motif), as per manufacturer's instructions, with reconstituted Jurkat cells were treated with 20 ng/mL PMA plus 300 ng/mL Ionomycin or 10 ng/mL TNFα during 30 min. For the RT^2 profiler PCR array of human NF-κB signaling targets, cells were treated with 20 ng/mL PMA plus 300 ng/mL Ionomycin or 10 ng/mL TNFα for 4h. RNA was extracted using the Nucleospin RNAplus kit (Macherey-Nagel), following manufacturer's instructions. 2 mg of RNA was reverse transcribed using the Maxima Reverse Transcriptase kit (ThermoFisher). RT^2 profiler PCR array of human NF-κB signaling targets was performed as instructed by the manufacturer (Qiagen).

Statistical analysis

Statistical analysis, comparing multiple groups was performed using two-way ANOVA on rank test with Tuckey's post hoc test in GraphPad Prism 7 software. TransAM NF-κB activation assays were analyzed using a 2-way ANOVA test with a Sidak correction for multiple analysis. RT^2 profiler PCR array was performed using the online software provided by the manufacturer (https://dataanalysis2.qiagen.com/pcr). In short, the p-values were calculated based on a student t-test of the replicate 2^(-DC_T) values for each gene in the control group and treatment group. The p-value calculation used is based on a parametric, unpaired, two sample equal variance, two tailed distribution. P-values < 0.05 were considered as significant.

Acknowledgments

This research was funded by an International Program for Scientific Cooperation (PICS, CNRS), Fondation pour la Recherche Médicale (Equipe labellisée DEQ20180339184),

bioRxiv preprint doi: https://doi.org/10.1101/2020.07.02.184085; this version posted July 3, 2020. The copyright holder for this preprint (which was not certified by peer review) is the author/funder. All rights reserved. No reuse allowed without permission.

Fondation ARC contre le Cancer (NB), Ligue nationale contre le cancer comités de Loire-Atlantique, Maine et Loire, Vendée (JG, NB), Région Pays de la Loire et Nantes Métropole under Connect Talent Grant (JG), the National Research Agency under the Programme d'Investissement d'Avenir (ANR-16-IDEX-0007), and the SIRIC ILIAD (INCa-DGOS-Inserm_12558). AT and SR hold post-doctoral fellowships from la Fondation ARC contre le Cancer. TD is a PhD fellow funded by Nantes Métropole. This work was also supported by grants from Biogenouest, Infrastructures en Biologie Santé et Agronomie (IBiSA) and Conseil Régional de Bretagne awarded to CP.

Author contribution

An Thys: Conceptualization, Methodology, Formal analysis, Investigation, Writing – original draft, Visualization, Funding acquisition. Kilian Trillet, Sara Rosinska, Audrey Gayraud, Tiphaine Douanne, Clotilde Renaud, Luc Antigny and Régis Lavigne: Investigation.
Yannic Danger and Franck Vérité: Resources. Emmanuelle Com: Methodology, Formal analysis, Investigation. Charles Pineau: Methodology. Julie Gavard: Writing – Review and Editing, Supervision, Funding acquisition. Nicolas Bidère: Conceptualization, Methodology, Investigation, Writing – original draft, Visualization, Funding acquisition

Conflict of interest

The authors declare that they have no conflict of interest.

bioRxiv preprint doi: https://doi.org/10.1101/2020.07.02.184085; this version posted July 3, 2020. The copyright holder for this preprint (which was not certified by peer review) is the author/funder. All rights reserved. No reuse allowed without permission.

References

1. Gerlach B, Cordier SM, Schmukle AC, Emmerich CH, Rieser E, Haas TL, Webb AI, Rickard JA, Anderton H, Wong WW-L, et al. (2011) Linear ubiquitination prevents inflammation and regulates immune signalling. *Nature* **471**: 591–596.
2. Ikeda F, Deribe YL, Skånland SS, Stieglitz B, Grabbe C, Franz-Wachtel M, van Wijk SJL, Goswami P, Nagy V, Terzic J, et al. (2011) SHARPIN forms a linear ubiquitin ligase complex regulating NF-κB activity and apoptosis. *Nature* **471**: 637–641.
3. Tokunaga F, Nakagawa T, Nakahara M, Saeki Y, Taniguchi M, Sakata S, Tanaka K, Nakano H, Iwai K (2011) SHARPIN is a component of the NF-κB-activating linear ubiquitin chain assembly complex. *Nature* **471**: 633–636.
4. Damgaard RB, Nachbur U, Yabal M, Wong WW-L, Fiil BK, Kastirr M, Rieser E, Rickard JA, Bankovacki A, Peschel C, et al. (2012) The Ubiquitin Ligase XIAP Recruits LUBAC for NOD2 Signaling in Inflammation and Innate Immunity. *Mol Cell* **46**: 746–758.
5. Hostager BS, Fox DK, Whitten D, Wilkerson CG, Eipper BA, Francone VP, Rothman PB, Colgan JD (2010) HOIL-1L Interacting Protein (HOIP) as an NF-κB Regulating Component of the CD40 Signaling Complex. *PLoS ONE* **5**: e11380.
6. Inn K-S, Gack MU, Tokunaga F, Shi M, Wong L-Y, Iwai K, Jung JU (2011) Linear Ubiquitin Assembly Complex Negatively Regulates RIG-I- and TRIM25-Mediated Type I Interferon Induction. *Mol Cell* **41**: 354–365.
7. Tokunaga F, Sakata S, Saeki Y, Satomi Y, Kirisako T, Kamei K, Nakagawa T, Kato M, Murata S, Yamaoka S, et al. (2009) Involvement of linear polyubiquitylation of NEMO in NF-κB activation. *Nat Cell Biol* **11**: 123–132.
8. Zak DE, Schmitz F, Gold ES, Diercks AH, Peschon JJ, Valvo JS, Niemisto A, Podolsky I, Fallen SG, Suen R, et al. (2011) Systems analysis identifies an essential role for SHANK-associated RH domain-interacting protein (SHARPIN) in macrophage Toll-like receptor 2 (TLR2) responses. *Proc Natl Acad Sci* **108**: 11536–11541.
9. Zhang M, Tian Y, Wang R-P, Gao D, Zhang Y, Diao F-C, Chen D-Y, Zhai Z-H, Shu H-B (2008) Negative feedback regulation of cellular antiviral signaling by RBCK1-mediated degradation of IRF3. *Cell Res* **18**: 1096–1104.
10. Kirisako T, Kamei K, Murata S, Kato M, Fukumoto H, Kanie M, Sano S, Tokunaga F, Tanaka K, Iwai K (2006) A ubiquitin ligase complex assembles linear polyubiquitin chains. *EMBO J* **25**: 4877–4887.
11. Iwai K, Fujita H, Sasaki Y (2014) Linear ubiquitin chains: NF-κB signalling, cell death and beyond. *Nat Rev Mol Cell Biol* **15**: 503–508.
12. Shimizu Y, Taraborrelli L, Walczak H (2015) Linear ubiquitination in immunity. *Immunol Rev* **266**: 190–207.
13. Karin M, Greten FR (2005) NF-κB: linking inflammation and immunity to cancer development and progression. *Nat Rev Immunol* **5**: 749–759.
14. Rickard JA, Anderton H, Etemadi N, Nachbur U, Darding M, Peltzer N, Lalaoui N, Lawlor KE, Vanyai H, Hall C, et al. (2014) TNFR1-dependent cell death drives inflammation in Sharpin-deficient mice. *eLife* **3**: e03464.
15. Peltzer N, Rieser E, Taraborrelli L, Draber P, Darding M, Pernaute B, Shimizu Y, Sarr A, Draberova H, Montinaro A, et al. (2014) HOIP Deficiency Causes Embryonic Lethality by Aberrant TNFR1-Mediated Endothelial Cell Death. *Cell Rep* **9**: 153–165.
16. Peltzer N, Darding M, Montinaro A, Draber P, Draberova H, Kupka S, Rieser E, Fisher A, Hutchinson C, Taraborrelli L, et al. (2018) LUBAC is essential for embryogenesis by preventing cell death and enabling haematopoiesis. *Nature* **557**: 112–117.
17. Satpathy S, Wagner SA, Beli P, Gupta R, Kristiansen TA, Malinova D, Francavilla C, Tolar P, Bishop GA, Hostager BS, et al. (2015) Systems-wide analysis of BCR signalosomes and downstream phosphorylation and ubiquitylation. *Mol Syst Biol* **11**: 810.
18. Teh CE, Lalaoui N, Jain R, Policheni AN, Heinlein M, Alvarez-Diaz S, Sheridan JM, Rieser E, Deuser S, Darding M, et al. (2016) Linear ubiquitin chain assembly complex

bioRxiv preprint doi: https://doi.org/10.1101/2020.07.02.184085; this version posted July 3, 2020. The copyright holder for this preprint (which was not certified by peer review) is the author/funder. All rights reserved. No reuse allowed without permission.

coordinates late thymic T-cell differentiation and regulatory T-cell homeostasis. *Nat Commun* **7**: 13353.

19. Yang Y, Schmitz R, Mitala J, Whiting A, Xiao W, Ceribelli M, Wright GW, Zhao H, Yang Y, Xu W, et al. (2014) Essential role of the linear ubiquitin chain assembly complex in lymphoma revealed by rare germline polymorphisms. *Cancer Discov* **4**: 480–493.
20. Dubois SM, Alexia C, Wu Y, Leclair HM, Leveau C, Schol E, Fest T, Tarte K, Chen ZJ, Gavard J, et al. (2014) A catalytic-independent role for the LUBAC in NF-kappaB activation upon antigen receptor engagement and in lymphoma cells. *Blood* **123**: 2199–2203.
21. Staudt LM, Dave S (2005) The Biology of Human Lymphoid Malignancies Revealed by Gene Expression Profiling. In, *Advances in Immunology* pp 163–208. Elsevier.
22. Thys A, Douanne T, Bidere N (2018) Post-translational Modifications of the CARMA1-BCL10-MALT1 Complex in Lymphocytes and Activated B-Cell Like Subtype of Diffuse Large B-Cell Lymphoma. *Front Oncol* **8**: 498.
23. Keusekotten K, Elliott PR, Glockner L, Fiil BK, Damgaard RB, Kulathu Y, Wauer T, Hospenthal MK, Gyrd-Hansen M, Krappmann D, et al. (2013) OTULIN Antagonizes LUBAC Signaling by Specifically Hydrolyzing Met1-Linked Polyubiquitin. *Cell* **153**: 1312–1326.
24. Heger K, Wickliffe KE, Ndoja A, Zhang J, Murthy A, Dugger DL, Maltzman A, de Sousa e Melo F, Hung J, Zeng Y, et al. (2018) OTULIN limits cell death and inflammation by deubiquitinating LUBAC. *Nature* **559**: 120–124.
25. Fuseya Y, Fujita H, Kim M, Ohtake F, Nishide A, Sasaki K, Saeki Y, Tanaka K, Takahashi R, Iwai K (2020) The HOIL-1L ligase modulates immune signalling and cell death via monoubiquitination of LUBAC. *Nat Cell Biol*.
26. Goto E, Tokunaga F (2017) Decreased linear ubiquitination of NEMO and FADD on apoptosis with caspase-mediated cleavage of HOIP. *Biochem Biophys Res Commun* **485**: 152–159.
27. Joo D, Tang Y, Blonska M, Jin J, Zhao X, Lin X (2016) Regulation of Linear Ubiquitin Chain Assembly Complex by Caspase-Mediated Cleavage of RNF31. *Mol Cell Biol* **36**: 3010–3018.
28. Lee IY, Lim JM, Cho H, Kim E, Kim Y, Oh H-K, Yang WS, Roh K-H, Park HW, Mo J-S, et al. (2019) MST1 Negatively Regulates TNFα-Induced NF-κB Signaling through Modulating LUBAC Activity. *Mol Cell* **73**: 1138-1149.e6.
29. Douanne T, Gavard J, Bidère N (2016) The paracaspase MALT1 cleaves the LUBAC subunit HOIL1 during antigen receptor signaling. *J Cell Sci* **129**: 1775–1780.
30. Elton L, Carpentier I, Staal J, Driege Y, Haegman M, Beyaert R (2016) MALT1 cleaves the E3 ubiquitin ligase HOIL-1 in activated T cells, generating a dominant negative inhibitor of LUBAC-induced NF-κB signaling. *FEBS J* **283**: 403–412.
31. Klein T, Fung S-Y, Renner F, Blank MA, Dufour A, Kang S, Bolger-Munro M, Scurll JM, Priatel JJ, Schweigler P, et al. (2015) The paracaspase MALT1 cleaves HOIL1 reducing linear ubiquitination by LUBAC to dampen lymphocyte NF-κB signalling. *Nat Commun* **6**: 8777.
32. Park Y, Jin H, Lopez J, Lee J, Liao L, Elly C, Liu Y-C (2016) SHARPIN controls regulatory T cells by negatively modulating the T cell antigen receptor complex. *Nat Immunol* **17**: 286–296.
33. Dubois SM, Alexia C, Wu Y, Fest T, Tarte K, Chen ZJ, Gavard J (2014) A catalytic-independent role for the LUBAC in NF-kB activation upon antigen receptor engagement and in lymphoma cells. **123**: 6.
34. Haas TL, Emmerich CH, Gerlach B, Schmukle AC, Cordier SM, Rieser E, Feltham R, Vince J, Warnken U, Wenger T, et al. (2009) Recruitment of the Linear Ubiquitin Chain Assembly Complex Stabilizes the TNF-R1 Signaling Complex and Is Required for TNF-Mediated Gene Induction. *Mol Cell* **36**: 831–844.
35. Thome M, Charton JE, Pelzer C, Hailfinger S (2010) Antigen Receptor Signaling to NF-B via CARMA1, BCL10, and MALT1. *Cold Spring Harb Perspect Biol* **2**: a003004–a003004.

bioRxiv preprint doi: https://doi.org/10.1101/2020.07.02.184085; this version posted July 3, 2020. The copyright holder for this preprint (which was not certified by peer review) is the author/funder. All rights reserved. No reuse allowed without permission.

36. Bonizzi G, Karin M (2004) The two NF-κB activation pathways and their role in innate and adaptive immunity. *Trends Immunol* **25**: 280–288.
37. Gilmore TD (2006) Introduction to NF-κB: players, pathways, perspectives. *Oncogene* **25**: 6680–6684.
38. De Franceschi N, Peuhu E, Parsons M, Rissanen S, Vattulainen I, Salmi M, Ivaska J, Pouwels J (2015) Mutually Exclusive Roles of SHARPIN in Integrin Inactivation and NF-κB Signaling. *PloS One* **10**: e0143423.
39. Pouwels J, De Franceschi N, Rantakari P, Auvinen K, Karikoski M, Mattila E, Potter C, Sundberg JP, Hogg N, Gahmberg CG, et al. (2013) SHARPIN regulates uropod detachment in migrating lymphocytes. *Cell Rep* **5**: 619–628.
40. Rantala JK, Pouwels J, Pellinen T, Veltel S, Laasola P, Mattila E, Potter CS, Duffy T, Sundberg JP, Kallioniemi O, et al. (2011) SHARPIN is an endogenous inhibitor of β1-integrin activation. *Nat Cell Biol* **13**: 1315–1324.
41. Dustin ML, Bromley SK, Kan Z, Peterson DA, Unanue ER (1997) Antigen receptor engagement delivers a stop signal to migrating T lymphocytes. *Proc Natl Acad Sci* **94**: 3909–3913.
42. Stoll S (2002) Dynamic Imaging of T Cell-Dendritic Cell Interactions in Lymph Nodes. *Science* **296**: 1873–1876.
43. Bousso P, Robey E (2003) Dynamics of CD8+ T cell priming by dendritic cells in intact lymph nodes. *Nat Immunol* **4**: 579–585.
44. Sun L, Wang H, Wang Z, He S, Chen S, Liao D, Wang L, Yan J, Liu W, Lei X, et al. (2012) Mixed Lineage Kinase Domain-like Protein Mediates Necrosis Signaling Downstream of RIP3 Kinase. *Cell* **148**: 213–227.
45. Yoon S, Kovalenko A, Bogdanov K, Wallach D (2017) MLKL, the Protein that Mediates Necroptosis, Also Regulates Endosomal Trafficking and Extracellular Vesicle Generation. *Immunity* **47**: 51-65.e7.
46. Elliott PR, Nielsen SV, Marco-Casanova P, Fiil BK, Keusekotten K, Mailand N, Freund SMV, Gyrd-Hansen M, Komander D (2014) Molecular Basis and Regulation of OTULIN-LUBAC Interaction. *Mol Cell* **54**: 335–348.
47. Elliott PR, Leske D, Hrdinka M, Bagola K, Fiil BK, McLaughlin SH, Wagstaff J, Volkmar N, Christianson JC, Kessler BM, et al. (2016) SPATA2 Links CYLD to LUBAC, Activates CYLD, and Controls LUBAC Signaling. *Mol Cell* **63**: 990–1005.
48. Seymour RE, Hasham MG, Cox GA, Shultz LD, Hogenesch H, Roopenian DC, Sundberg JP (2007) Spontaneous mutations in the mouse Sharpin gene result in multiorgan inflammation, immune system dysregulation and dermatitis. *Genes Immun* **8**: 416–421.
49. Davis RE, Brown KD, Siebenlist U, Staudt LM (2001) Constitutive Nuclear Factor κB Activity Is Required for Survival of Activated B Cell–like Diffuse Large B Cell Lymphoma Cells. *J Exp Med* **194**: 1861–1874.
50. Compagno M, Lim WK, Grunn A, Nandula SV, Brahmachary M, Shen Q, Bertoni F, Ponzoni M, Scandurra M, Califano A, et al. (2009) Mutations of multiple genes cause deregulation of NF-κB in diffuse large B-cell lymphoma. *Nature* **459**: 717–721.
51. Banliat C, Tsikis G, Labas V, Teixeira-Gomes A-P, Com E, Lavigne R, Pineau C, Guyonnet B, Mermillod P, Saint-Dizier M (2020) Identification of 56 Proteins Involved in Embryo–Maternal Interactions in the Bovine Oviduct. *Int J Mol Sci* **21**: 466.
52. Bouyssié D, Hesse A-M, Mouton-Barbosa E, Rompais M, Macron C, Carapito C, Gonzalez de Peredo A, Couté Y, Dupierris V, Burel A, et al. (2020) Proline: an efficient and user-friendly software suite for large-scale proteomics. *Bioinformatics* **36**: 3148–3155.
53. Savitski MM, Lemeer S, Boesche M, Lang M, Mathieson T, Bantscheff M, Kuster B (2011) Confident Phosphorylation Site Localization Using the Mascot Delta Score. *Mol Cell Proteomics* **10**: M110.003830.
54. Douanne T, André-Grégoire G, Trillet K, Thys A, Papin A, Feyeux M, Hulin P, Chiron D, Gavard J, Bidère N (2019) Pannexin-1 limits the production of proinflammatory cytokines during necroptosis. *EMBO Rep* **20**:.

bioRxiv preprint doi: https://doi.org/10.1101/2020.07.02.184085; this version posted July 3, 2020. The copyright holder for this preprint (which was not certified by peer review) is the author/funder. All rights reserved. No reuse allowed without permission.

Figure legends

Figure 1. SHARPIN is a Phosphoprotein.

A Jurkat cells were treated with or without 50 nM Calyculin A (Cal A) for 30 min prior lysis. Cell lysates from primary human $CD4^+$ or $CD8^+$ T lymphocytes and Jurkat cells were treated with lambda phosphatase (λPP) as indicated, and subjected to Western blotting analysis. Green and white arrowheads indicate phosphorylated and unphosphorylated SHARPIN, respectively. Molecular weight markers (M_r) are indicated.

B Densitometric analysis of the ratio between phosphorylated species of SHARPIN and SHARPIN in primary human T $CD4^+$ cells, primary human T $CD8^+$ T cells, Jurkat T cells, a panel of patient-derived diffuse large B-cell lymphoma cell lines, HeLa and MCF-7 cells.

C-D Primary human $CD4^+$ T (E) and $CD8^+$ T lymphocytes (F), and Jurkat cells (G) were stimulated for 30 min or as indicated with 20 ng/mL PMA plus 300 ng/mL ionomycin (PI). Lysates were prepared and treated or not with λPP and Western blotting analysis was performed as indicated.

E Jurkat cells were stimulated with 20 ng/mL PMA, 300 ng/mL ionomycin, PMA plus ionomycin (PI), 10 ng/mL TNFα or 12.5 µg/mL Anisomycin, for 30 min. Cell lysates were subjected to Western blotting analysis.

F Jurkat cells we pretreated for 1h with 1 µM Trametinib or 500 nM BIMVIII and subsequently stimulated and lysed as in (E). Blue arrowhead indicates HOIL-1 Cter.

Figure 2. The Serine Residue of SHARPIN in Position 165 is a major Phosphorylation Site.

A Mass spectrometry analysis of immunoprecipitates prepared from Jurkat cell lysates with antibodies to SHARPIN identified phosphorylation sites. The identified peptides

bioRxiv preprint doi: https://doi.org/10.1101/2020.07.02.184085; this version posted July 3, 2020. The copyright holder for this preprint (which was not certified by peer review) is the author/funder. All rights reserved. No reuse allowed without permission.

were validated with an FDR < 1% and a minimum score of 30. The peptide score calculated in the Mascot search engine following $-10\log_{10}(p)$, where p is the absolute probability. The position of the post-translational modification in the protein (PTM), the modification site probability calculated in Proline (site probability) the number of peptides identified, the peptide sequence with the identified amino acid in blue the localization and other amino acid modifications in green.

B Sequence alignment of the amino acids surrounding the serine (S) 129, S131, S146, S165 and S312 residues.

C Jurkat cells knockout for *Sharpin* were engineered by CRISPR/Cas9. Cells were complemented with an empty vector (EV), or with wild-type (WT), S165A-, S312A- or S165A plus S312A (2SA)-SHARPIN. Cells were stimulated for 30 min with antibodies to CD3 and CD28 (1 µg/mL each). Cell lysates were prepared and subjected to Western blotting analysis. White and green symbols show SHARPIN and phosphorylated SHARPIN, respectively. Molecular weight markers (M_r) are indicated.

D *Sharpin* knockout Jurkat cells reconstituted with EV, WT- or S165A-SHARPIN were treated with PI as in (C), or with 10 ng/mL TNFα. Cells lysates were Immunoprecipitated (IP) with antibodies specific to SHARPIN and subjected to Western blotting analysis with a mouse antibody specific for p-S165-SHARPIN.

E Cell lysates from *Sharpin* knockout Jurkat cells reconstituted with an empty vector (EV), wild-type (WT-) or S165A-SHARPIN were subjected to Western blotting analysis with antibodies specific to the indicated antibodies.

F Cell lysates from EV, WT-, S165A- or S165D-SHARPIN reconstituted *Sharpin* knockout Jurkat cells were submitted to SHARPIN immunoprecipitation (IP) prior to western blotting analysis for LUBAC components. * indicates the heavy chain of the SHARPIN antibody used for IP.

Figure 3: Serine 165 Phosphorylation of SHARPIN is crucial for the optimal Activation of NF-κB.

bioRxiv preprint doi: https://doi.org/10.1101/2020.07.02.184085; this version posted July 3, 2020. The copyright holder for this preprint (which was not certified by peer review) is the author/funder. All rights reserved. No reuse allowed without permission.

A *Sharpin* knockout Jurkat cells expressing an empty vector (EV) or wild type (WT-), S165A- or S165D-SHARPIN were stimulated with 10 ng/mL TNFα for 24 h. Cell viability was assessed with CellTiter glo (mean ± SEM; ***P<0.001 by two-way ANOVA).

B WT- and S165A-expressing Jurkat cells were stimulated with 10 ng/mL TNFα as indicated. Cell lysates were subjected to immunoprecipitation (IP) of linear ubiquitin (M1) prior to Western blotting analysis with the specified antibodies. Molecular weight markers (M_r) are indicated.

C *Sharpin* knockout Jurkat cells expressing an empty vector (EV) or wild type (WT-) or S165A-SHARPIN were stimulated with 20 ng/mL PMA plus 300 ng/mL ionomycin (PI) or CD3 plus CD28 (1 µg/mL each) for 30 min. Cell lysates were subjected to western blotting analysis. Blue symbol indicates HOIL-1 Cter cleavage band.

D NF-κB reporter luciferase assay in the indicated Jurkat cells treated for 6 h with 20 ng/mL PMA plus 300 ng/mL ionomycin (PI), 1 µg/mL anti-CD3 plus 1 µg/mL anti-CD28, or with 1 ng/mL TNFα. Graph displays 1 out of 3 experiments done in triplicate (mean ± SEM; *p<0.05, **P<0.01 by two-way ANOVA).

E WT- or S165A-SHARPIN reconstituted Jurkat cells were stimulated with PI or TNFα for 30 min as in (D) before performing TransAM NF-κB activation assay for p65 and p50 NF-κB subunits. The presented Graph show 1 out of 3 experiment performed in duplicate (mean ± SEM; *p<0.05, **P<0.01 by two-way ANOVA).

F-G Volcano plot or RT^2 profiler PCR array of human NF-κB signaling targets for cells stimulated for 4 h with PI (F) or TNFα (H). (G) Genes indicated on the volcano plot are significantly down regulated with a fold change > 2 in cells expressing S165A-SHARPIN when compared to WT-SHARPIN. On (G), CXCR2 is significantly down regulated with a fold change >2, while other genes indicated are borderline significant in S165A-SHARPIN expressing cells, compared to WT-SHARPIN. (F-G) Heatmap in

bioRxiv preprint doi: https://doi.org/10.1101/2020.07.02.184085; this version posted July 3, 2020. The copyright holder for this preprint (which was not certified by peer review) is the author/funder. All rights reserved. No reuse allowed without permission.

the below volcano plot gives an overall view of the gene expression in the RT^2 profiler PCR array.

Expanded View Figure legends

Figure EV1, relative to Figure 1 SHARPIN Phosphorylation by ERK upon Antigen Receptor Engagement.

A Western blotting analysis of a panel of patient-derived diffuse large B-cell lymphoma (DLBCL) cell lines. Cell lysates were treated with lambda phosphatase (λPP) as indicated, and subjected to Western blotting analysis. Green and white arrowheads indicate phosphorylated and unphosphorylated SHARPIN, respectively. Molecular weight markers (M_r) are indicated.

B Primary peripheral blood mononuclear cells (PBMC) were stimulated with 12.5 µg/mL Anisomycin, 20 ng/mL PMA, 300 ng/mL ionomycin, PMA plus ionomycin or 10 ng/mL TNFα for 30 min. Cell lysates were subjected to Western blotting analysis.

C Jurkat cells were pretreated with 1 µM Trametinib (MEK1/2 inhibitor), 500 nM Bisindolylmaleimide VIII (BIMVIII) (PKC inhibitor), 1 µM, 50 µM SP6000125 (JNK inhibitor), or 5 µM SB203580 (p38 inhibitor), and subsequently treated with CD3 plus CD28 (1µg/µL each). Western blotting analysis was performed as indicated. Treatment with SB203580 gave non-specific results as it also regulated ERK phosphorylation. Yellow symbol indicates CYLD Cter cleavage band.

D HEK293T cells were co-transfected with plasmids encoding for HOIP, SHARPIN or HOIP plus SHARPIN together with ERK1-FLAG. Cells were lysed with TNT. Cell lysates were immunoprecipitated using anti-FLAG M2 affinity gel and subjected to Western blotting analysis.

E The LUBAC was pulled down by immunoprecipitation of Jurkat cell lysates using the HOIL-1 antibody. *In vitro* kinase assay was performed by adding active ERK1, ERK2-GST or ERK1 plus ERK2-GST recombinant proteins to HOIL-1 pulled down beads.

bioRxiv preprint doi: https://doi.org/10.1101/2020.07.02.184085; this version posted July 3, 2020. The copyright holder for this preprint (which was not certified by peer review) is the author/funder. All rights reserved. No reuse allowed without permission.

677 Western blotting analysis was performed for the indicated antibodies. White and
678 green arrows show SHARPIN and phosphorylated SHARPIN, respectively. Molecular
679 weight markers (M_r) are indicated.
680
681 **Figure EV2, relative to Figure 2. Characterization of SHARPIN knockout Cells**
682 A SHARPIN identified during mass spectrometry analysis (peptide rank1, peptide score
683 > 30, FDR<1% at PSM level). The protein score is the sum of the unique peptide
684 score calculated following $-10\log_{10}(p)$, where p is the absolute probability. Peptide
685 count and spectral count are indicated.
686 B Mass spectrometry analysis of immunoprecipitates prepared from Jurkat cell lysates
687 with antibodies to SHARPIN identified phosphorylation sites. The identified peptides
688 were validated with an FDR < 1% and a minimum score of 30. The peptide score
689 calculated in the Mascot search engine following $-10\log_{10}(p)$, where p is the absolute
690 probability. The position of the post-translational modification in the protein (PTM), the
691 number of peptides identified, the peptide score, the peptide sequence with the
692 modified amino acid in blue the localization confidence value of the post-translational
693 modification calculated in the Mascot search engine (ptm sites confidence) and the
694 number of spectra detected for each peptide (#PSM or peptide-spectrum match).
695 C Scheme showing the sgRNA target and PAM site on SHARPIN for the LentiCRISPR
696 vector containing SHARPIN sgRNA.
697 D Western blotting analysis of Jurkat single cell clones targeted with sgSHARPIN
698 LentCRISPRv2 (knock down, KD or an empty vector (EV).
699 E Jurkat *Sharpin* KO cells were complemented with an empty vector (EV), or with wild-
700 type (WT), S165A-, S312A- or S165A+S312A (2SA)-SHARPIN. Cells were stimulated
701 for 30 min with 20 ng/mL PMA plus 300 ng/mL ionomycin. Cell lysates were
702 subjected to Western blotting analysis. White and green symbols show SHARPIN and
703 phosphorylated SHARPIN, respectively. Molecular weight markers (M_r) are indicated.

bioRxiv preprint doi: https://doi.org/10.1101/2020.07.02.184085; this version posted July 3, 2020. The copyright holder for this preprint (which was not certified by peer review) is the author/funder. All rights reserved. No reuse allowed without permission.

F NF-κB reporter luciferase assay of Parental Jurkat and Jurkat knockout (KO) cells treated for 6 h with 20 ng/mL PMA plus 300 ng/mL ionomycin, CD3 plus CD28 (1 µg/mL each) or 1 ng/mL TNFα (mean ± SEM; *p<0.05, **P<0.01 by one-way ANOVA, n=2).

G Cell lysates from Jurkat, *Sharpin* KO Jurkat cells or cells reconstituted with EV, WT-, S165A- or S165D-SHARPIN. Western blotting analysis was performed for the indicated proteins.

Figure EV3, relative to Figure 3.

A-B Jurkat cells (A) or *Sharpin* knockout (KO) Jurkat cells, reconstituted with wild type (WT-) or S165A-SHARPIN (B) were stimulated with 100 ng/mL TNFα-FLAG for the indicated time points.). Cell lysates were immunoprecipitated using anti-FLAG M2 affinity gel (A-B). Beads were incubated with or without lambda phosphatase (λPP) (A) and subjected to Western blotting analysis (A-B). White and green symbols show SHARPIN and phosphorylated SHARPIN, respectively. Molecular weight markers (M_r) are indicated.

C-D Cell lysates of WT- and S165A-expressing Jurkat were treated with 10 ng/mL TNFα (C) or with 20 ng/mL PMA plus 300 ng/mL ionomycin (PI) (D) as indicated and subjected to Western blotting analysis.

E WT- or S165A-SHARPIN reconstituted Jurkat cells were stimulated with PI or TNFα for 30 min as in (B-C) before performing TransAM NF-κB activation assay for cREL NF-κB subunit. (mean ± SEM; *p<0.05, **P<0.01 by two-way ANOVA, n=2).

F-G List of RT^2 profiler PCR array of human NF-κB signaling targets with an expression fold change >2 in in cells expressing S165A-SHARPIN when compared to WT-SHARPIN. Cells were treated during 4h with 20 ng/mL PMA plus 300 ng/mL ionomycin (F) or 10 ng/mL TNFα (G). Fold regulation and p-value are listed.

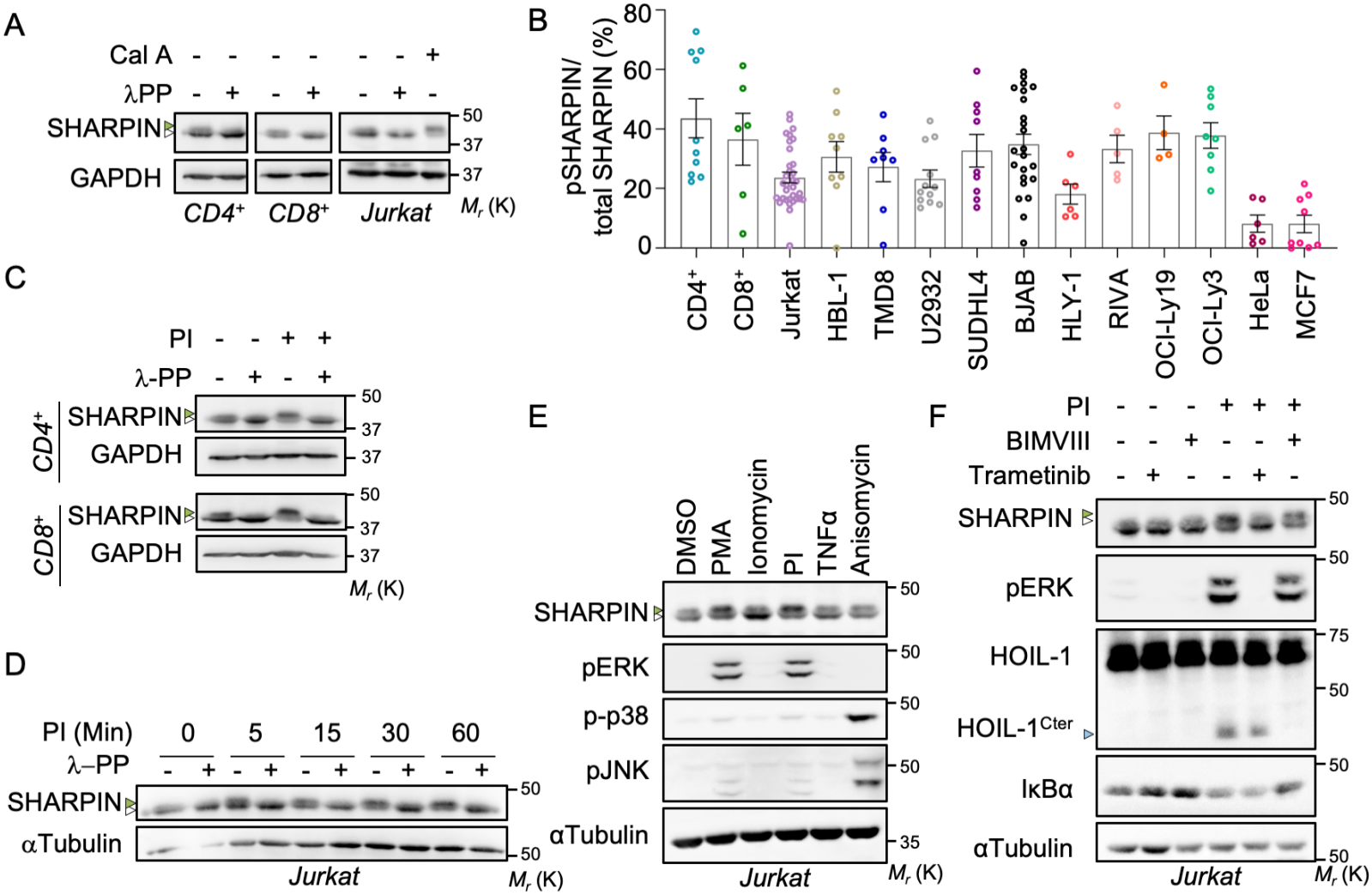
A
Cal A
λPP
SHARPIN
GAPDH
CD4+
CD8+
Jurkat
Mr (K)
B
pSHARPIN/ total SHARPIN (%)
CD4+
CD8+
Jurkat
HBL-1
TMD8
U2932
SUDHL4
BJAB
HLY-1
RIVA
OCI-Ly19
OCI-Ly3
HeLa
MCF7
C
PI
λ-PP
SHARPIN
GAPDH
D
PI (Min)
λ–PP
SHARPIN
αTubulin
E
DMSO
PMA
Ionomycin
PI
TNFα
Anisomycin
SHARPIN
pERK
p-p38
pJNK
αTubulin
F
PI
BIMVIII
Trametinib
SHARPIN
pERK
HOIL-1
HOIL-1Cter
IκBα
αTubulin

A

PTM Protein Position	Site Probability	Pep. No.	Sequence
Phospho S129	65,20%	1	SNSPPALGPEACPVS LPSPPEASTLK
		2	SNSPPALGPEACPVS LPSPPEASTLK
Phospho S131	50%	1	SNSPPALGPEACPVS LPSPPEASTLK
		2	SNSPPALGPEACPVS LPSPPEASTLK
Phospho S146	92.44%	3	SNSPPALGPEACPVS LPSPPEASTLK
		2	SNSPPALGPEACPVS LPSPPEASTLK
		2	SNSPPALGPEACPVS LPSPPEASTLK
Phospho S165	100%	4	SPGNLTER
Phospho S312	89.49%	5	EAPATGPSPQHPQK

B

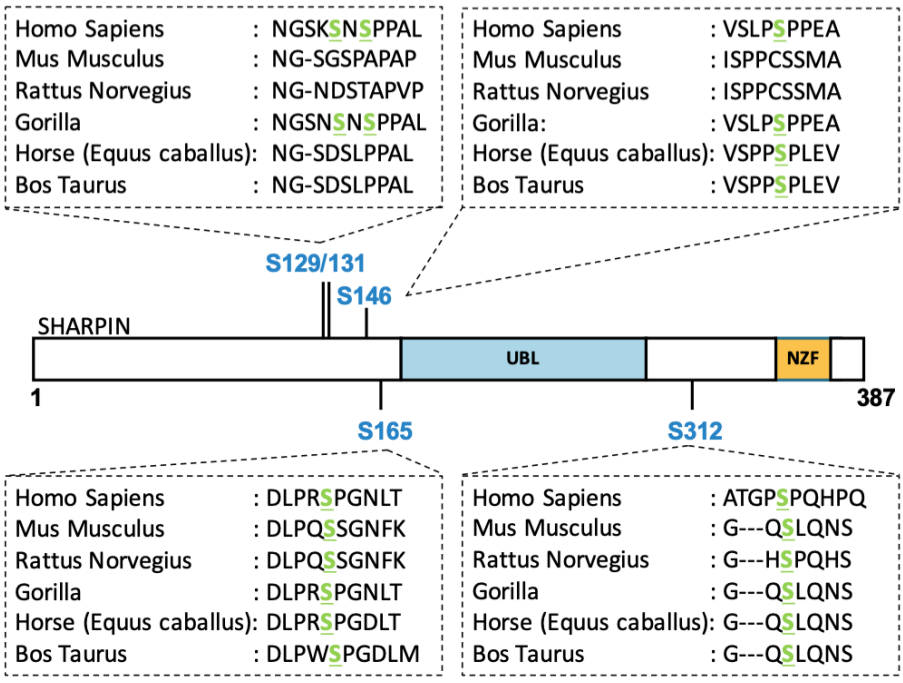

C

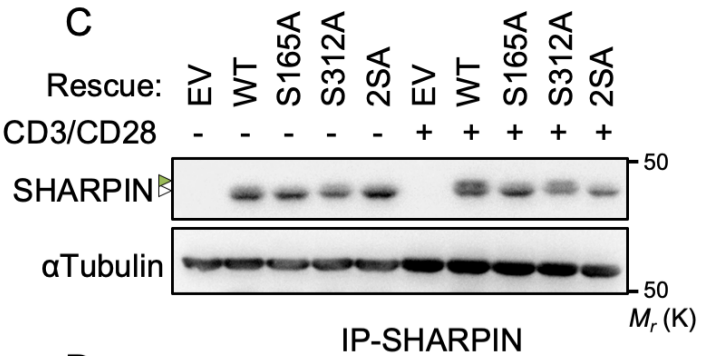

D

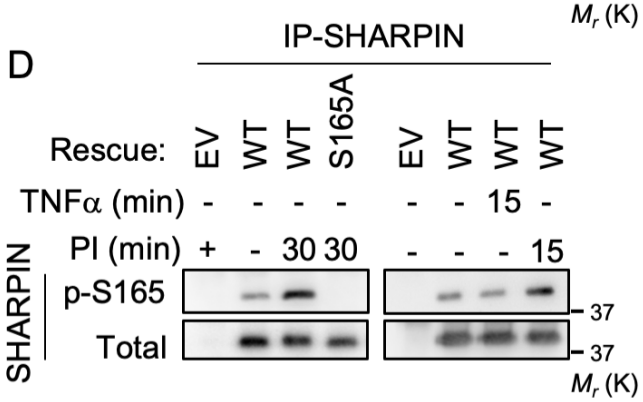

E

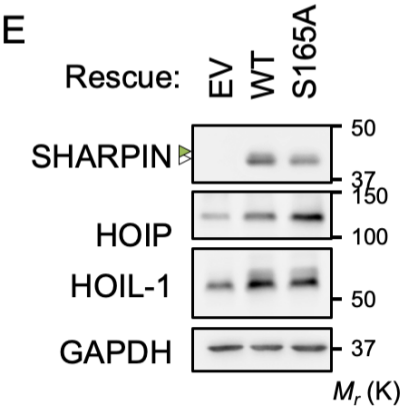

F

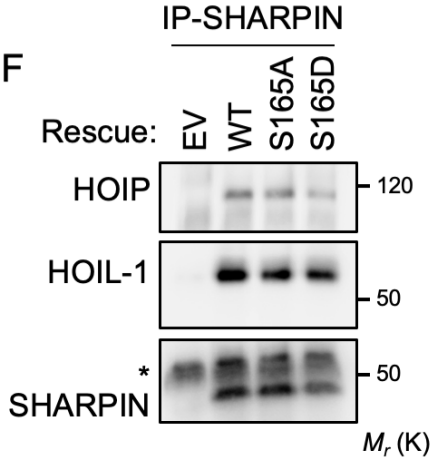

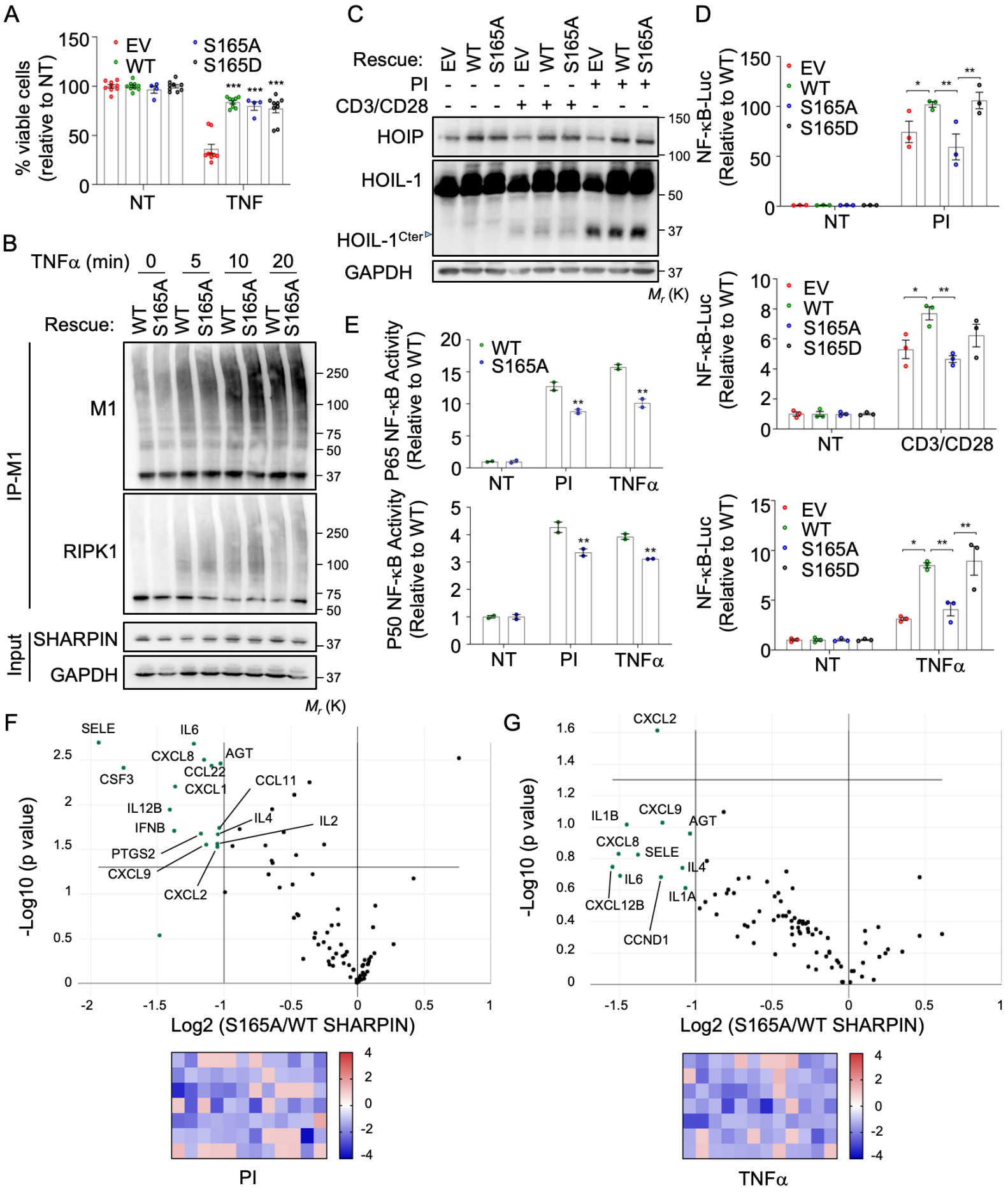
A
% viable cells (relative to NT)
EV
WT
S165A
S165D
NT
TNF
B
TNFα (min)
Rescue:
IP-M1
M1
RIPK1
Input
SHARPIN
GAPDH
Mr (K)
C
Rescue:
PI
CD3/CD28
HOIP
HOIL-1
HOIL-1Cter
GAPDH
Mr (K)
D
NF-κB-Luc (Relative to WT)
NT
PI
CD3/CD28
TNFα
E
P65 NF-κB Activity (Relative to WT)
P50 NF-κB Activity (Relative to WT)
NT
PI
TNFα
F
-Log10 (p value)
Log2 (S165A/WT SHARPIN)
SELE
IL6
CXCL8
AGT
CSF3
CCL22
CXCL1
CCL11
IL12B
IL4
IL2
IFNB
PTGS2
CXCL9
CXCL2
PI
G
-Log10 (p value)
Log2 (S165A/WT SHARPIN)
CXCL2
IL1B
CXCL9
AGT
CXCL8
SELE
IL4
IL6
IL1A
CXCL12B
CCND1
TNFα

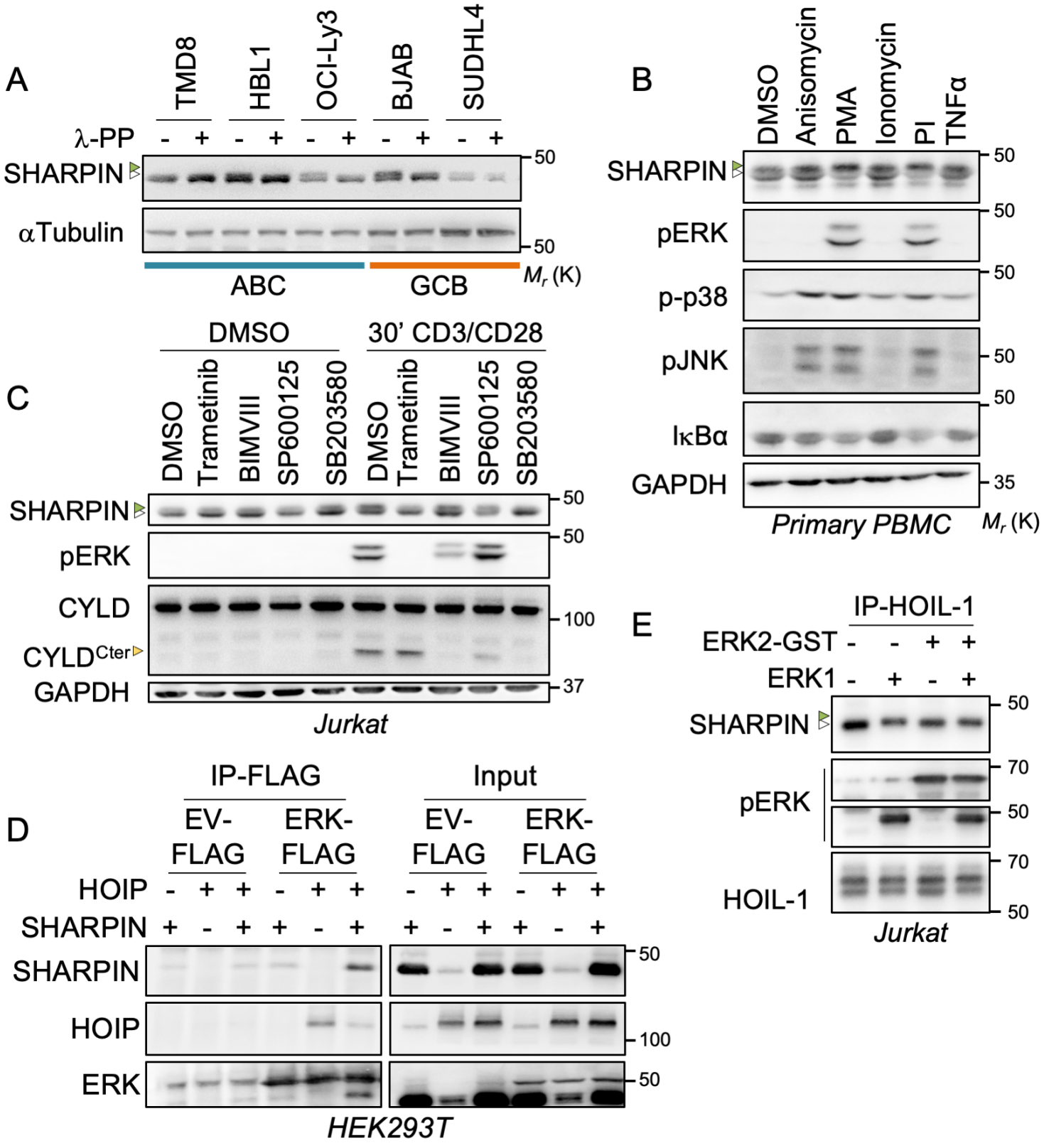
A
TMD8
HBL1
OCI-Ly3
BJAB
SUDHL4
λ-PP - + - + - + - + - +
SHARPIN
αTubulin
50
50
ABC
GCB
Mr (K)
B
DMSO
Anisomycin
PMA
Ionomycin
PI
TNFα
SHARPIN
pERK
p-p38
pJNK
IκBα
GAPDH
50
50
50
50
50
35
Primary PBMC
Mr (K)
C
DMSO
30' CD3/CD28
DMSO
Trametinib
BIMVIII
SP600125
SB203580
SHARPIN
pERK
CYLD
CYLDCter
GAPDH
50
50
100
37
Jurkat
D
IP-FLAG
Input
EV-FLAG
ERK-FLAG
HOIP - + + - + + - + + - + +
SHARPIN + - + + - + + - + + - +
SHARPIN
HOIP
ERK
50
100
50
HEK293T
E
IP-HOIL-1
ERK2-GST - - + +
ERK1 - + - +
SHARPIN
pERK
HOIL-1
50
70
50
70
50
Jurkat

A

Protein set	Description	Score	Peptides	Spectral Count
Sp/Q9H0F6/SHRPN_HUMAN	Sharpin OS=Homo sapiens (Human) OX=9606 GN=SHARPIN PE=1 SV=1	1048.03	20	61

B

PTM Protein Position	Pep. No.	Score	Sequence	PTM Sites Confidence	#PSM
Phospho S129	1	49.06	SNSPPALGPEACPVSLPSPPEASTLK	Phospho (S1) = 50%	3
	2	61.81	SNSPPALGPEACPVSLPSPPEASTLK	Phospho (S1) = 50% Phospho (S18) =92%	2
Phospho S131	1	49.06	SNSPPALGPEACPVSLPSPPEASTLK	Phospho (S3) = 50%	3
	2	61.81	SNSPPALGPEACPVSLPSPPEASTLK	Phospho (S3) = 50% Phospho (S18) = 92%	1
Phospho S146	3	44.59	SNSPPALGPEACPVSLPSPPEASTLK	Phospho (S18) = 91%	1
	2	61.81	SNSPPALGPEACPVSLPSPPEASTLK	Phospho (S1) = 50% Phospho (S18) = 92%	2
	2	61.81	SNSPPALGPEACPVSLPSPPEASTLK	Phospho (S3) = 50% Phospho (S18) = 92%	1
Phospho S165	4	41.63	SPGNLTER	Phospho (S1) = 100%	2
Phospho S312	5	38.87	EAPATGPSPQHPQK	Phospho (S8) = 89%	1

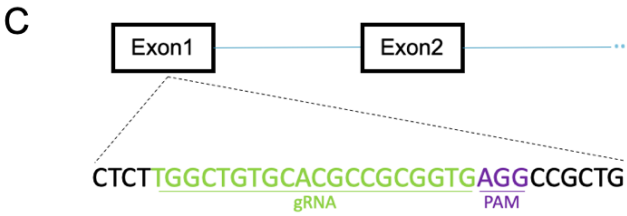

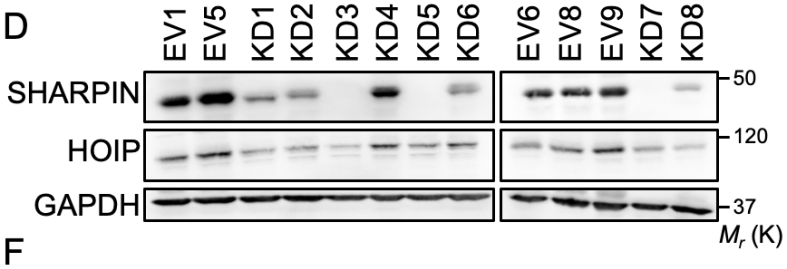

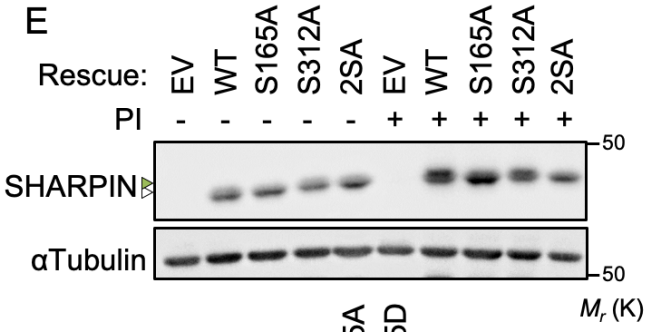

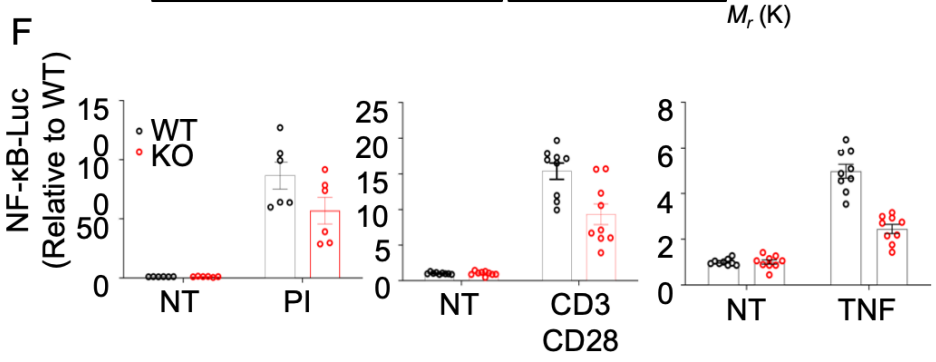

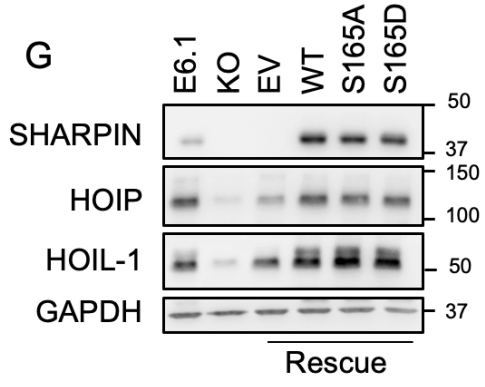

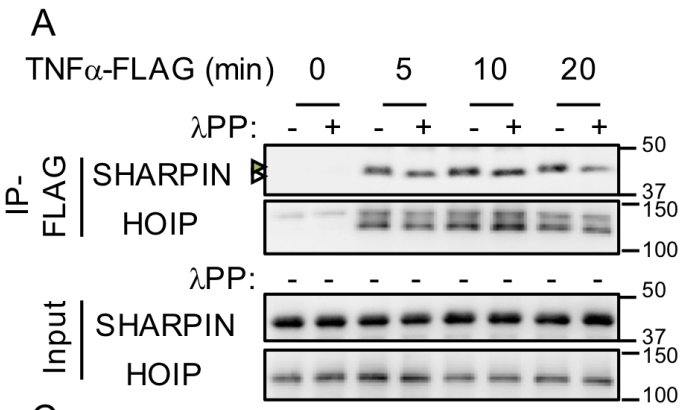

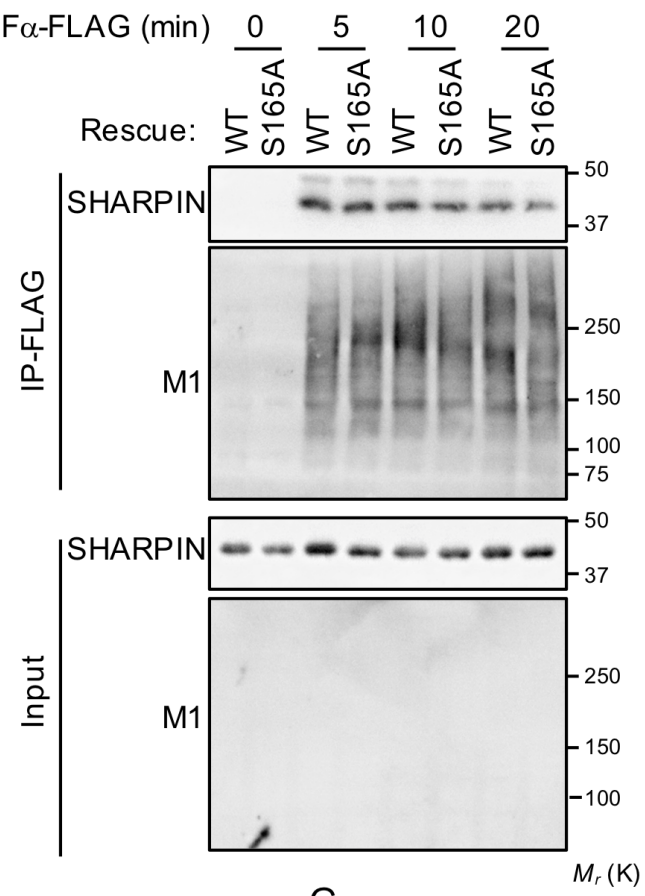

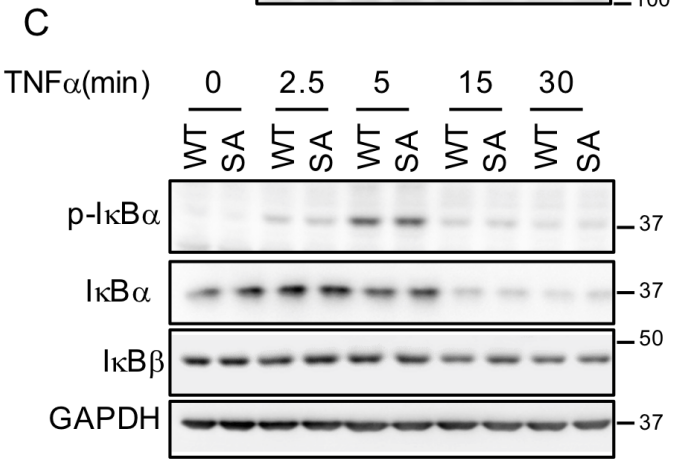

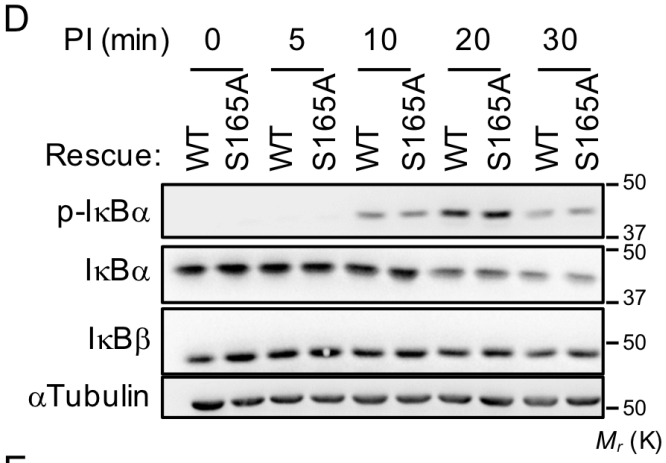

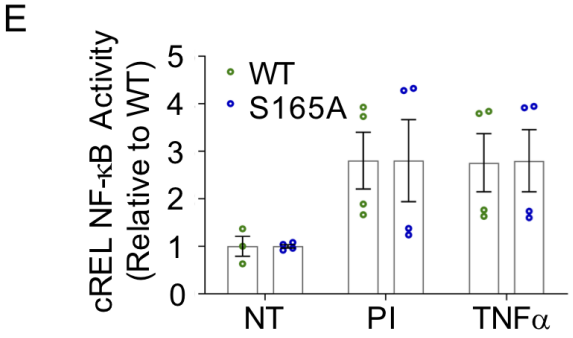

F

Gene Symbol	Fold regulation	P value
SELE	-3.84	0.002010
CSF3	-3.37	0.003848
IL12B	-2.65	0.011335
IFNB1	-2.59	0.019553
CXCL1	-2.58	0.006250
IL6	-2.34	0.002069
PTGS2	-2.26	0.021027
CXCL8	-2.22	0.003132
CXCL9	-2.19	0.027996
CCL22	-2.13	0.003650
CXCL2	-2.07	0.029537
IL2	-2.07	0.027333
IL4	-2.07	0.021390
CCL11	-2.05	0.018191
AGT	-2.04	0.003451

G

Gene Symbol	Fold regulation	P value
CXCL2	**-2.38**	**0.024300**
IL12B	-2.92	0.178692
CXCL8	-2.83	0.147931
IL6	-2.82	0.203720
IL1B	-2.73	0.096160
SELE	-2.60	0.149616
CCND1	-2.34	0.207953
CXCL9	-2.32	0.093671
IL4	-2.12	0.181482
IL1A	-2.09	0.243840
AGT	-2.05	0.109868